Mapping of Au geochemical anomalies using logratio-transformed stream sediment geochemical data in 1:100000 Feyzaabad sheet, Khorasan Razavi, Iran

Farzaneh Zandiyyeh and Mohammad Reza Shayestehfar

Mining Engineering Department, Shahid Bahonar University, Kerman, Iran.

Abstract

In the present study, analyses of log- and logratio-transformation of stream geochemical data of Au in 1:100000 Feyzaabad sheet are compared with each other. Logratio (alr, clr, or ilr) transformations, compared to log-transformation, of stream sediment geochemical data improve mapping of Au anomalies which indicates presence of mineralization. Particularly, the anomaly maps of Au derived from clr- or ilr-transformed stream sediment geochemical data are better, than the anomaly maps of Au derived from log- or alr-transformed data. The results of the study suggest that stream sediment geochemical data in the study area should be clr- or ilr- transformed to enhance recognition of anomalous multi-element associations reflecting the presence of mineralization. The enhancement of anomalous multi-element associations is the most important benefit of either clr- or ilr-transformation compared to either ln- or alr-transformation of stream sediment geochemical data.

Keywords: Compositional data; Log-ratio transformations; Concentration-area plots; Au anomalies; Feyzaabad; Iran.

1. Introduction

There are high mineral potentials and a multitude of discovered minerals in Iran. One of the gold and copper mineralization areas in Iran is the study area in 1:100,000 Feyzaabad sheet, East of Iran, located in the eastern continuation of Taknar mineralization zone, and is bounded by Darouneh and Rivash faults (Heydari, 2011). In the study area, various kinds of mineralization can be seen that may or may not be accompanied by gold mineralization with different concentrations. The mineralization is generally formed of specularite + quartz + chalcopyrite + pyrite + malachite + hematite + gold (Heydari, 2011).

Quantity evaluation of chemical constituents of earth materials in order to find controlling parameters for elemental distributions has been carried out in the geochemistry (Goldschmidt, 1937). A classical example for a closed array or closed number system is a data set in which the individual variables are not independent of each other but are related by being expressed as a percentage or parts per million (Filzmoser et al., 2009a; Reimann et al., 2012). Compositional data have been explained as summing up to a constant, but nowadays they have a broader explanation, as they are considered to be a part of the whole data which only include relative information (Buccianti and Pawlowsky-Glahn, 2005; Pawlowsky-Glahn and Egozcue, 2006).

In the last five decades, various researchers have discussed the conflicts in statistical analysis of closed number systems such as compositional data sets (Aitchison, 1981, 1983, 1984, 1986, 1999; Aitchison et al., 2000; Egozcue et al., 2003; Buccianti and Pawlowsky-Glahn, 2005; Egozcue and Pawlowsky-Glahn, 2005; Thió-Henestrosa and Martín-Fernández, 2005; Filzmoser et al., 2009a, 2009b; Carranza 2011; Wang et al., 2014). For opening closed number systems, three logratio transformations have been suggested: (1) additive logratio (alr) transformation (Aitchison, 1986), (2) centered logratio (clr) transformation (Aitchison, 1986) (3) isometric logratio (ilr) transformations (Egozcue et al., 2003). In addition, Filzmoser et al. (2009b) discussed that, except for the three logratio transformations which are suggested for opening of close number systems, any other transformation of compositional variables is not effective.

Several software packages have been proposed (Thió-Henestrosa and Martín-Fernández, 2005; Van den Boogaart and Tolosana-Delgado, 2009) and have prepared

for the public (R Development Core Team, 2008; Templ et al., 2009) for proper analysis of compositional data. Thus, with the establishment of the mathematical formalism and public accessibility of software for compositional data analysis, practitioners and scientists in the field of exploration should no longer follow improper procedures for analysis and mapping of geochemical anomalies for mineral exploration (Carranza, 2011).

However, in spite of the significant progress in addressing the conflicts in statistical analyses of closed number systems, the log-ratio transformations in order to open the closed number systems are still rarely applied for analysis and mapping of geochemical anomalies for mineral exploration. Many researchers, in the field of geochemical exploration for data normality still usually apply a log or natural log (ln) transformation. Therefore, to demonstrate and document that the developments in compositional data analysis are beneficial in mineral exploration, several inspections and investigations are in order. The objective of this study is to investigate the following question.

- Does log-ratio (i.e.,alr, clr and ilr) transformation, in comparison with log transformation of stream sediment geochemical data improve interpretation and mapping of anomalies representing the presence of mineralization?

1.1. Geology of study area

Feyzaabad sheet by scale of 1:100000 is located in Khorasan Razavi province in the east of Iran. The study area is located in the central part of Khaf-Bardaskan volcanic-plutonic belt (Mazloumi et al., 2008), between two major faults: Darouneh in the south and Taknar (Rivash) in the north. Both the faults are of slip-strike type and have an approximate east-west trend (Heydari, 2011). This belt is also introduced as Taknar (Eftekharnezhad et al., 1976; Lindenberg et al., 1983). Different researchers in their investigations, described the ore bodies which are located in this belt, meanwhile according to geochemical and geological indicators, they found that the aforementioned belt has certain geological and magmatism conditions that caused Au mineralization (Mazloumi et al., 2008). Four considerable gold mineralizations were recognized in the study area (Exploration Co. Jiangxi, 1994; Heydari, 2011; Shahi and Kamkar-Rouhani, 2014) (Fig. 1). The Taknar mineralization belt is underlain by Precambrian and Paleozoic basement, and overlain by Mesozoic and Cenozoic cover. There are facial and structural differences between this zone and adjacent zones.

Cambrian strata is exposed only in the southwest of the region, the main lithologies are limestone, dolomite, shale and sandy shale. The exposed Ordovician district is the same as that of Cambrian where the main lithologies are shale and siltstone (Fig. 1). The exposed Silurian district closely adjoins that of Ordovician, the lithologies of the lower part are thin bedded limestone and shale and the upper part are sandstone, dolomite with gypsum. Devonian is exposed only in south west of the region (Fig. 1). The lithologies of the lower part are black dolomite and shale while that of the upper part are limestone and dolomitic limestone. Jurassic is mainly exposed in the north-eastern part of the study area where the lithologies are dolomitic limestone, limestone, marl and shale. Cretaceous is extensively distributed in the northern part of the region. The lithologies of the lower part are sandstone and conglomerate while of the upper part has Globotruncana limestone. Tertiary can be divided in to two parts (Paleogene and Neogene) (Fig. 1).

Paleogene is exposed in the central part and the northern part of the region characterized by volcanic rocks, whose lithologies are andesite, tuff, pyroxene andesite, trachyte, tuffaceous breccia, sandstone, marl, limestone and conglomerate. Neogene is exposed in the southern part of the region characterized by clastic rocks, whose main lithologies are conglomerate, sandstone, siltstone, marl with gypsum and a little volcanic clastic rock (Behrouzi, 1987). Quaternary is mainly distributed in the recent alluvial area such as intermountainous basin and river bed. Its lithologies are sand, gravel and clay. The structure of this region is dominated by the
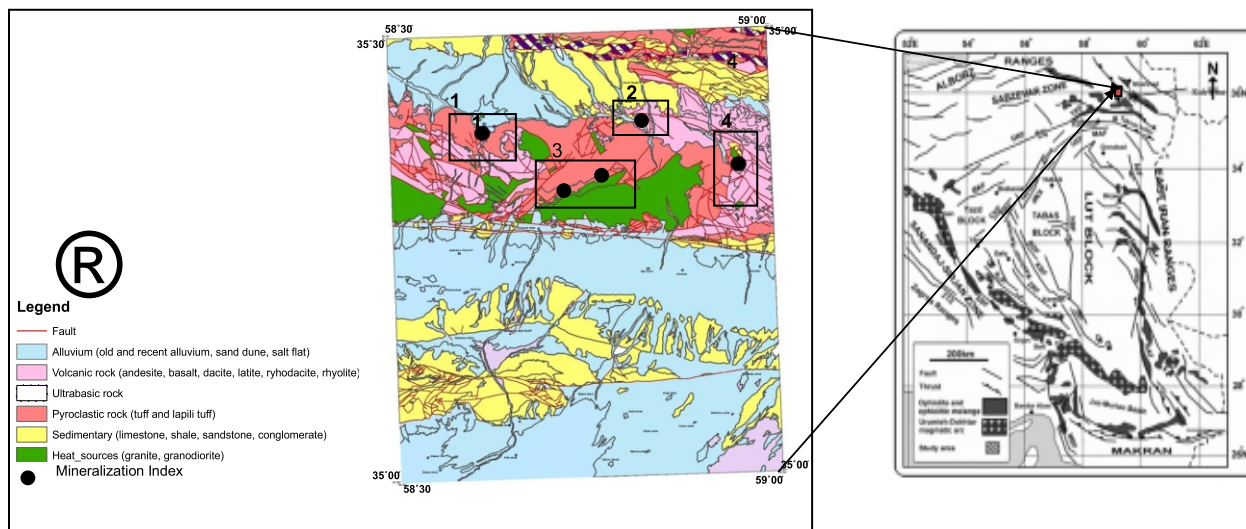
Fig.1. Geological map of 1:100000 Feyzaabad sheet and its situation in the structural map of Iran (Behrouzi, 1987; Stöcklin, 1968).

fractures; the folded structure often appears as anticline, being cut by the fractures with small and short scale. The distribution of the strata and magmatic rock were controlled by the faulted structure which is intercalated with N-W and E-W trending structures. Two major faulted structures in south and north are Kavir and Northern faulted structure. The first one is located in the southwestern part with N-W trending; the faulted structure is an east-extending part of Doruneh inner-arc deep fracture projection towards north. The distribution of Tertiary volcanic island arc and acid magmatic rocks were controlled by the north wall while the deposition of Upper Tertiary clastic sediments was taken by the south wall (Fig.1). The Northern faulted structure is located in the northwestern part. Trending from WE to NW, the structure controls the distribution of serpentinite, basic and ultrabasic rocks, being ore-controlling and rock-controlling structures (Fig.1). Acid and intermediate-acid intrusive rocks are extensively exposed in the northern regional large fracture, its main lithologies are granite and granodiorite, diorite and dacite vein can be observed in many places. Serpentinite is controlled by E-W- trending faults is extensively exposed in northern edge of the region (Fig. 1).

2. Methodology

2.1. Stream sediment geochemical data

Actual sampling area of the case study in

the whole sheet is 2066 Km^2. In the study area, there is data set for 1033 composite basic samples of -40 mesh (0.44 mm) fraction of stream sediments. (Exploration Co. Jiangxi, 1994). The collected samples were analyzed for 28 elements. A complete set of analytical methods of samples were selected to fit the daily analysis for a great amount of samples and meet the requirements of geochemical mapping and they had high productive efficiency. Only seven elements (Au, Cu, Zn, Ag, As, Sb, Hg) are discussed here. In order to fit the daily analysis for a great amount of samples and meet the requirements of geochemical mapping, the selected analytical methods and detection limits should be of high productive efficiency. The concentration of Au in the samples i.e., detected by Spectroscopy with chemical enrichment (Es-I) method (Exploration Co. Jiangxi, 1994). The concentrations of Cu and Zn elements were determined using inductively coupled plasmas atomic emission spectroscopy (ICP) method (Exploration Co. Jiangxi, 1994). Ag concentration was determined by atomic emission spectroscopy (ES) method (Exploration Co. Jiangxi, 1994). Also, the concentrations of As, Sb and Hg elements were detected by atomic fluorescence spectroscopy (AFS) method (Exploration Co. Jiangxi, 1994). The detection limits of Au, Cu, Zn, Ag, As, Sb, Hg were 0.0003, 1, 10, 0.02, 0.2, 0.1, 0.02 ppm. Statistical results reveal that mean values of Au, Cu, Zn, Ag, As, Sb, Hg are 1.522 ppb, 1.046 ppm, 1.074 ppm, 1.043 ppm, 1.084 ppm, 1.077 ppm and 1.076 ppm respectively (Table 1). In stream sediment geochemical

exploration, regardless of chemical pollution, the variation from the normal form, have two syngenetic and epigenetic components where the syngenetic component is related with petrogenesis and epigenetic component is related to economical mineralization that is known as the explorative useful component. Enrichment index is mainly independent of petrographic variations and reduces the random errors. So generally it is used for the elimination of petrographical effects (Hasanipak and Sharafaldin, 2004). After calculating the enrichment index for different rock communities in Feyzaabad sheet, the resulted data are integrated with each other and they are considered as one statistical community. The studied elements are helpful in mapping of remarkable anomalies that are associated with Au deposits.

2.2. Data transformations

In order to eliminate the spurious relationships between compositions, the family of logratio-transformations is used to deal with the closure effects. In practice, these transformations are commonly employed in geochemical data processing to open closed systems for better understanding of realistic relationships among compositions (Egozcue et al., 2003; Carranza, 2011; Filzmoser et al., 2012; Wang et al., 2014). In this study, the data were then transformed using log, alr, clr and ilr. Equation (11) of Filzmoser et al. (2009b) was used for ilr-transformation in order to univariate analysis. For multivariate analysis, Eq. (4) of Fizmoser et al. (2009b) was applied for ilr-transformation of uni-element data. Figure 3 shows the probability plots for raw and transformed (log, alr, clr, ilr) Au data in stream sediment samples. The probability plots of transformed Au data (Fig. 2a-d) are more symmetric than probability plot of raw Au data

(Fig. 2f). Thus, because of using compositional data, the logratio-transformed variable, cause a proper presentation of the data in Euclidean space, has to be applied for the Empirical Cumulative Distribution Function (ECDF) plot.

2.3. Spatial representation of stream sediment geochemical data

Visualizing the structure of the spatial data on a map is one of the major goals of geochemistry in regional scale (Reimann, 2005). Various methods have been applied successfully for mapping geo-chemical data and defining the thresholds (upper limit range of background values) in exploration geochemistry and distinguishing anthropogenic versus natural sources of materials (Nazarpour et al., 2015). In this study, the spatial interpolated maps by inverse distance weighting (IDW) method were used to portray anomalies. This method is applied with 12 neighboring samples used for estimation of each grid point. IDW is a moving-average interpolation method established upon the hypothesis that the values of neighboring data contribute more to interpolated values than the values of distance data (Hosseini et al., 2014). The merit of the IDW method is that it is instinctive and its implementation is uncomplicated. Its main drawback is related to the weight evaluations based only on the location and disregarding the variance of the values (Zuo, 2011).

2.4. Analysis and mapping of geochemical anomalies

The separation of geochemical anomalies from background in areas where the concentration of elements reveals a potential economic interest is a major objective in the

Table 1. Statistical parameters of studied elements based on stream sediment samples.

Statistical parameters	Au (ppb)	Cu (ppm)	Zn (ppm)	Ag (ppm)	As (ppm)	Sb (ppm)	Hg (ppm)
Mean	1.522	1.046	1.074	1.043	1.084	1.077	1.076
Median	1	1	1	1	1	1	1
Standard deviation	2.692	0.332	0.327	0.4	0.396	0.514	0.549
Maximum	45.377	4.925	4.056	8.25	5.313	6.818	12.54
Minimum	0.272	0.337	0.426	0.144	0.386	0.236	0.25

analysis and interpretation of geochemical data.. For the past many years, the traditional statistical methods presumed that the concentration of chemical elements in the crust follow a normal or log-normal distribution. It is demonstrated that the spatial position is a characteristic of geochemical data, which means that the concentration of element has spatial variation. However, the traditional methods accentuate the importance of only the frequency distribution of the elemental concentration, but the second group concentrates the spatio-statistical distribution of geochemical values, for example, geostatistical techniques, fractal methods, etc. Classical statistical methods are popular frequency based methods and widely used in many fields. The main limitation of the classical approach is that they do not consider the spatial information, geometry (e.g., shape or form), extent and magnitude of anomalous areas (Cheng et al., 1994) and may fail to recognize anomalies in regions with high-value background or miss weak anomalies in region with known mineral deposits (Bai et al., 2010; Hassanpour and Afzal, 2013; Nazarpour et al., 2015).The fractal theory is one of the non-linear mathematical methods that was established by Mandelbrot (1983) and widely used in many scientific fields including geosciences (e.g., Turcotte, 1986; Agterberg et al., 1993; Sim et al., 1999;Cheng et al.,1994; Carranza, 2008; Deng et al., 2010; Sadeghi et al., 2012; Hosseini et al., 2014; Nazarpour et al., 2015).
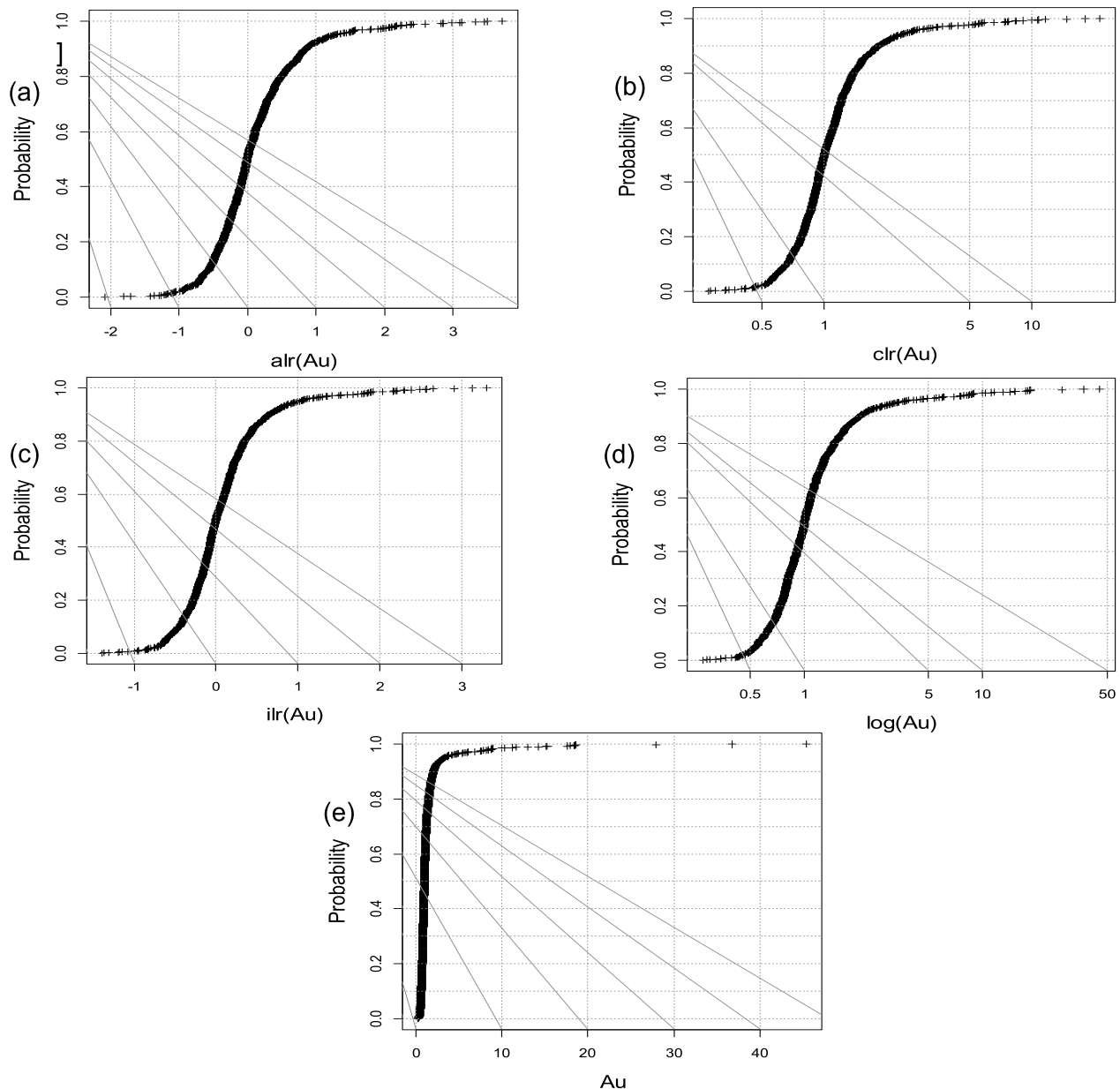

Fig.2. Probability plots of raw and transformed (log, alr, clr, ilr; a-d) and raw (e) Au data in stream sediment samples in 1:100000 Feyzaabad sheet.

In this study, the concentration-area (C-A) fractal analysis (Cheng et al., 1994, 1996, 1997, 2000) was adapted for separating background and anomalies uni-element and multi-element data (Hosseini et al., 2014; Daya and Afzal, 2015). The method has the general form as follow:

$$A(\rho \leq \upsilon) \propto \rho^{-a_1}; A(\rho \geq \upsilon) \propto \rho^{-a_2} \quad (1)$$

Where $A(\rho)$ denotes the area with concentration values greater than the contour value ρ, υ represents the threshold, and a_1 and a_2 are characteristic exponents. The breaks between straight line segments in C-A log-log plot and the corresponding values of ρ are known as thresholds. They are useful to separate ore concentration values into different components representing different casual factors such as lithological differences and geochemical processes and mineralizing events (Lima et al., 2003). The C-A method uses to display the relationship between element concentration values and geological data. The most useful feature of the C-A method is its capability to compute anomaly threshold (Afzal et al., 2010; Sadeghi et al., 2012; Rahmati et al., 2014; Hosseini et al., 2014).

For mapping of anomalies representing multi-element associations, the transformed datasets were individually input to principal component analysis (PCA). A PCA examination of this data set should cause more comprehensive understanding the relations between the variables and the geochemical processes controlling the element distribution in the study area. It is useful to display the loadings and scores together in biplots (Gabriel, 1971). The interpretation of the biplot depends on the chosen scale for loadings and scores. For the special interpretation of biplots for compositional data in the clr space we refer to the results of Aitchison and Greenacre (2002). A representation of the PCA results in biplots (Gabriel, 1977) results an accurate interpretation of the relations between compounds. The maps of the first view PCs scores represents the areas with specific higher or lower concentrations as a result of some significant geochemical processes. Although Filzmoser et al. (2009a) emphasized that ln transformation of single variables is not sufficient for multivariate analysis, the log-transformed uni-element data were also used in

PC analysis for the purpose of comparison only in order to answer the question raised in the introduction. The scores of a PC interpreted to reflect the presence of mineralization are subjected to the C-A fractal analysis to classify and map anomalies representing multi-element associations.

2.5. Comparison of anomalies

To answer the question raised in the introduction, the results of C-A analyses are converted into binary geochemical background-anomaly maps. Resulted maps are compared with reference map (Fig.3) of "ground-truth" which shows presence/absence of geochemical anomalies because of certain occurrences of mineral deposits (Carranza, 2011). This map was created by assigning a label of "anomaly" to samples that contain each of the known Au deposits in the study area and by assigning a label of "background" to the remaining data.

Each binary geochemical-anomaly map is intersected with the map of ground-truth presence/absence of geochemical anomalies. This operation of crossing two binary maps is a map with four overlap conditions, in which the numbers of data can be used to measure efficiency and performance of binary geochemical anomaly mapping.

In this study, the numbers of data of overlap conditions between two binary anomaly-background maps are used to determine overall accuracy and type I and type II errors (Carranza, 2011). Overall accuracy (denoted as OA) relates to the ability of the analysis to map background and anomalous areas. Type I error (denoted as T1E) relates to the ability of the transformation for the background mapping and it is computed as below:

T1E=False background(C)/ (True anomaly (A) + False background(C))

Type II error (denoted as T2E) relates to the ability of the transformation for anomaly mapping and it is computed as below:

T2E=False anomaly (B)/ (False anomaly (B) + True background (D))
OA= (A+D)/ (A+B+C+D)

If both types of errors are lower or OA is higher, the analysis ability for background and anomaly mapping area will be higher (Carranza, 2011). The calculated values of errors and accuracy chiefly depend to the type of data transformation. A lower T2E is more critical than a lower T1E because based on the former, the decision to explore for nothing would be made. Thus, the single factor applied for comparing the performance of the anomaly maps obtained in this study is the value of OA. The higher will be this value, the better will be an anomaly map which indicates that an anomaly map has a lower T2E as compared to T1E (Carranza, 2011).

3. Discussions

3.1. Anomaly maps of Au

The C-A plots of log-, alr, clr- and ilr-transformed Au data indicate two inflection points, showing that the datasets can be divided into three classes (Fig. 4). Considering the known epithermal –Au deposit occurrences, these three classes exhibit background, low

anomaly, and high –anomaly (Fig.4). The anomaly maps which are obtained from the log-, alr-, clr- and ilr- transformed Au data are quite similar to each other (Fig.4). The high anomalous regions in the anomaly maps are in accordance with the known gold mines and deposits. These anomalous areas have a good overlap with the E-W and NE-SW trending faults and the intrusive and volcanic rocks (Fig. 4). These suggest that all of different transformed Au data result in optimum mapping of anomalies using the C-A fractal analysis. For comparison with the ground-truth anomaly map (Fig.3), the low- and high-anomaly classes are re-classified into anomaly class. The OAs of the log- and alr-transformed Au data is lower than clr- and ilr-transformed Au data (Table 2). The values of OA for anomaly maps based on log-,alr-,clr- and ilr-transformed Au data are 0.83, 0.65,0.87 and 0.86, respectively (Table 2). These indicate that clr-transformed Au data are optimal for mapping of anomalies using the C-A fractal analysis.
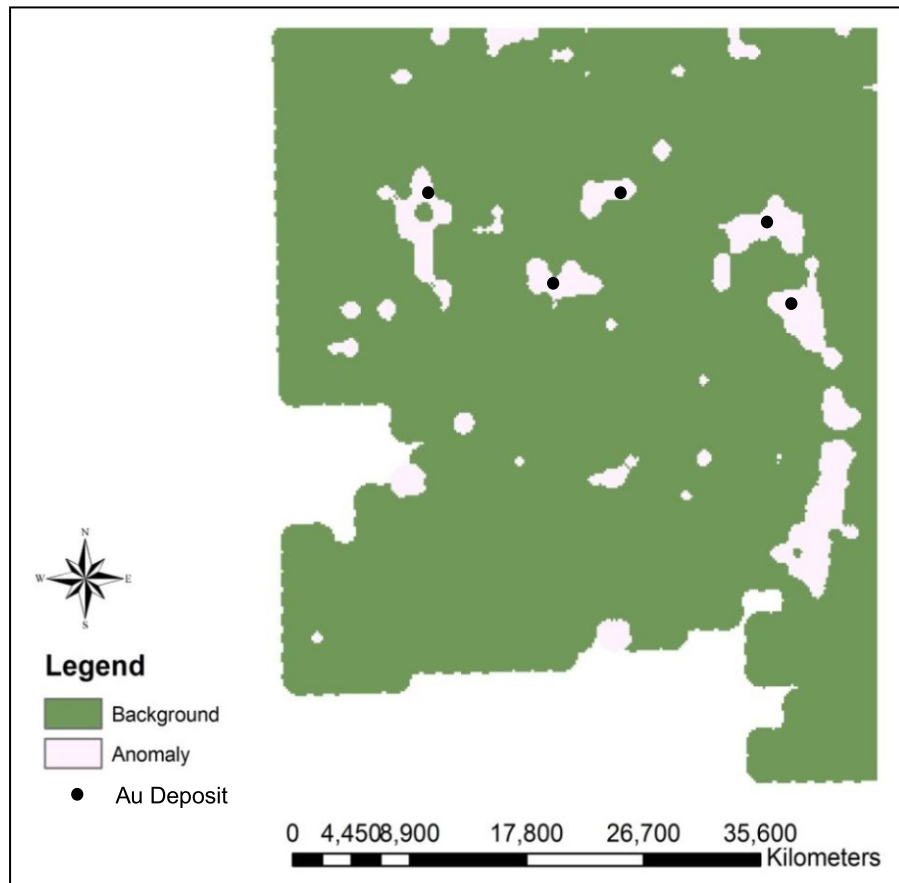

Fig.3. Binary map indicating Au anomalous regions and Au background regions in 1:100000 Feyzaabad sheet.

Table 2. Overall accuracy, Type I and Type II errors with respect to ground-truth background-anomaly map (Fig.3) of binary background-anomaly maps obtained from analysis of ln-, alr-, clr- and ilr-transformed Au data. Values in the matrix are number of samples of overlap condition between two binary anomaly-background maps.

log-transformed Au		Ground-truth		alr-transformed Au			Ground-truth	
		Anomaly	Background				Anomaly	Background
Results of analysis	Anomaly	47	158	Results of analysis	Anomaly		43	63
	Background	21	807		Background		25	902
	T1E=0.31	T2E=0.16			T1E=0.37		T2E=0.065	
	OA=0.83				OA=0.91			

clr-transformed Au		Ground-truth		ilr-transformed Au			Ground-truth	
		Anomaly	Background				Anomaly	Background
Results of analysis	Anomaly	44	60	Results of analysis	Anomaly		51	61
	Background	23	906		Background		24	897
	T1E=0.34	T2E=0.058			T1E=0.32		T2E=0.068	
	OA=0.92				OA=0.92			

3.2. Element associations

Principal component analysis (PCA) is one of the most significant and useful multivariate statistical procedures (Filazmoser et al., 2009a). This method vastly used for pre-process and dimension reduction of data, and the PCs are then applied for plotting or for subsequent multivariate analyses (Filazmoser et al., 2009a). A PCA analysis of the studied data set results in a better understanding of the relations among the variables and the controlling geochemical processes of the element distribution in the survey area. Biplots which simplify result visualization result in an accurate interpretation of the compounds relationships, and maps of the first view PCs indicate the areas with certain higher or lower concentrations because of some remarkable geochemical processes (Carranza, 2011).

In this study, the PCA results of the log- alr- clr- and ilr transformed data are compared with each other. The results of the ilr transformed data, back-transformed to the clr space are applied for compositional biplots.

PCs of the log- and alr- transformed data are strongly similar by considering the elemental associations and percentages of total variances in the respective datasets (Table 3). PC1 of log-transformed data represent statistically significant negative correlations between all elements except Hg which account for at least 61% of total variance in individual datasets. These results infer the presence of lurking variables. Because opening of closed number systems makes it possible in regard to all the variables, even if not all variables have been measured, the negative correlations between all elements in PC1 of either log- or alr-transformed data are artificial.

Therefore, log-transformation of stream sediment geochemical data, are insufficient for showing multi-element associations that could be worth looking in to for mineral exploration. Also, the strong resemblance of the PC1 of alr-transformed data with the PC1 of log-transformed data shows that alr-transformation is ineffective for opening compositional data (stream sediment geochemical data).
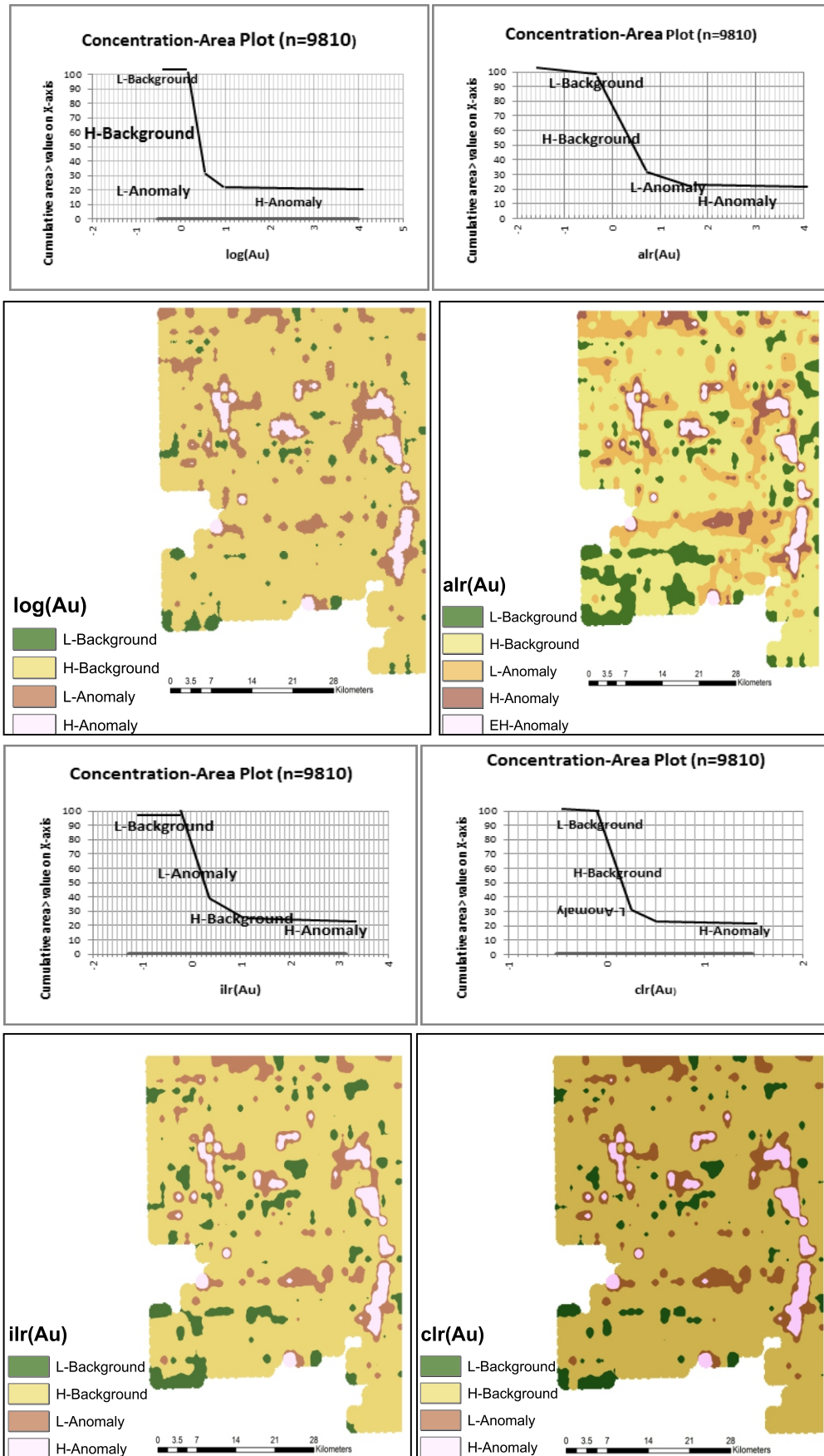
Fig. 4. Concentration-area plots of ln-, alr-, clr-, and ilr-transformed Au data and the
corresponding classified Au maps according to inflection points of concentration-area
plots (solid dots) along straight-line segments fitted through the plots. L=low, H=high.

93

Table 3. Rotated PCs of log-, alr-, clr- and ilr-transformed stream sediment geochemical data. Loadings in bold represent statistically significant eigenvector coefficients.

	Au	Cu	Zn	Ag	As	Sb	Hg	Eigen-value	% of variance
log-transformed data									
PC1	**-0.271**	**-0.186**	**-0.493**	**-0.364**	**-0.487**	**-0.528**	0.029	3.402	61.11
PC2	**0.481**	**0.602**	0.031	0.014	**-0.314**	**-0.248**	**0.491**	0.854	15.47
PC3	0.012	-0.49	-0.247	**0.461**	0.014	0.027	**0.687**	0.671	12.05
PC4	**-0.43**	0.149	0.232	**-0.62**	0.136	0.235	0.53	0.514	8.52
PC5	**0.619**	-0.203	-0.455	-0.471	0.321	0.206	0.017	0.254	2.85
alr-transformed data									
PC1	**-0.322**	**-0.402**	**-0.495**	**-0.406**	**-0.42**	**-0.328**	**-0.325**	3.402	61.17
PC2	**0.312**	**0.389**	-0.143	0.1	**-0.381**	**-0.606**	**0.467**	0.853	15.48
PC3	**0.851**	0.165	-0.208	**-0.153**	0.025	0.158	**-0.424**	0.67	12.11
PC4	**0.783**	-0.13	-0.495	-0.301	0.153	0.105	0.014	0.514	8.55
PC5	0.027	0.296	0.115	**-0.863**	0.029	0.287	0.263	0.255	2.69
clr-transformed data									
PC1	**0.436**	**0.289**	-0.33	-0.107	**-0.502**	**-0.517**	**0.295**	2.257	41.25
PC2	**0.595**	-0.468	-0.412	-0.191	0.025	**0.253**	-0.388	1.798	29.36
PC3	-0.103	-0.441	-0.327	**0.779**	0.041	-0.166	0.232	1.054	18.54
PC4	0.213	0.205	0.353	0.461	-0.23	-0.199	**-0.695**	0.689	9.52
PC5	0.045	-0.474	0.485	0.037	**-0.646**	0.25	0.229	0.254	1.33
ilr-transformed data									
PC1	**-0.821**	**-0.189**	0.164	0.147	**0.339**	**0.357**	0.005	2.897	45.82
PC2	**0.337**	-0.217	-0.016	-0.216	0.247	**0.533**	-0.668	1.653	26.56
PC3	-0.033	0.111	-0.021	**-0.846**	0.099	0.24	0.45	1.036	16.25
PC4	-0.201	0.592	0.574	0.215	-0.192	-0.138	**-0.421**	0.621	8.36
PC5	-0.022	-0.094	0.099	0.121	**-0.796**	0.561	0.131	0.145	3.01

PC2 represents a Cu-Hg-Au association which is likely because of gold mineralization and As-Sb association.

The PC1-PC2 biplots (Fig. 5) for log- and alr-transformed data show clearly the typical data closure problem. They are largely limited to a cramped half-circle. They represent strong correlations between all elements and two main element associations, namely Au-Cu-Hg and Zn-Ag-Sb-As (Fig. 5). PC3 shows an Ag-Hg association for both log- and alr-transformed data and also Au for alr-transformed data. In Table 3, PC4 of log-transformed data show Au-Ag negative associations and for alr-transformed data shows Au-As association. Finally PC5 for log-transformed data shows Au which reflects Au anomalies which are likely due to gold mineralization and for alr-transformed data shows Ag anomalies (Table 3).

The clr- and ilr- transformed data yield PCs that are strongly similar in terms of element associations and percentages of the total variances in respective datasets (Table 3). The clr- and ilr-transformed data, produced three PCs with eigenvalues >1 (Table 3).

Therefore, the results show that that either clr- or ilr-transformation is effective for opening closed number systems and is sufficient for showing multi-element associations that could be of interest in mineral exploration. In Table 3, PC1 shows Au-Cu-Hg and As-Sb associations. PC2 shows Au-Sb associations which reflect Au mineralization. The PC1-PC2 biplots (Fig. 5) for clr- and ilr-transformed data show that the data are now opened because the bias due to data closure has disappeared. They show four main element associations, namely Au, Sb-As, Hg-Cu and Zn-Ag (Fig. 5). In Table 3, PC3 reflects Ag anomalies that can indicate Au mineralization as a pathfinder element for gold deposits. PC4 shows Cu-Zn-Ag association and Hg anomalies and PC5 reflects Au anomalies, which are likely due to gold mineralization.
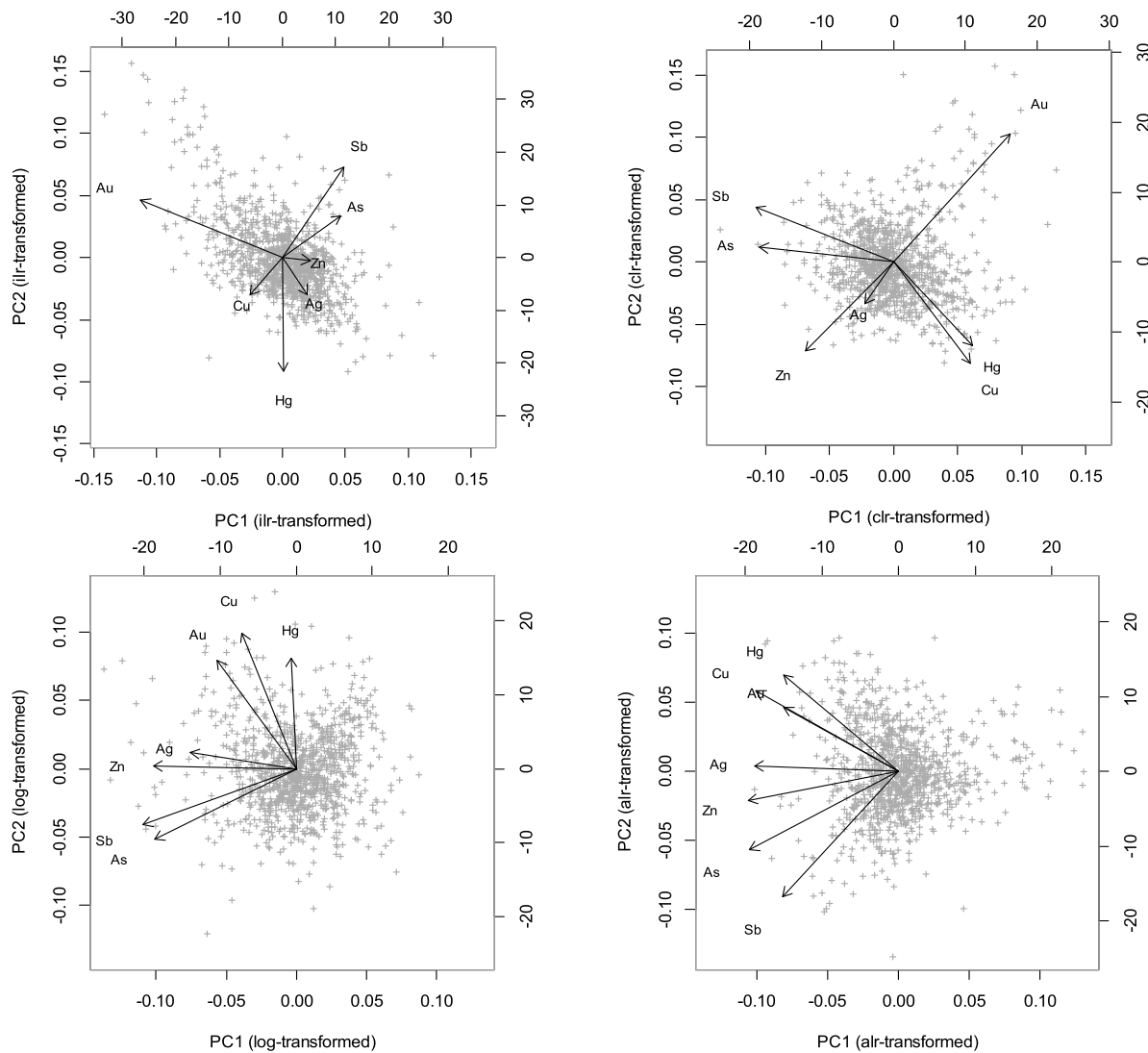
Fig.5. Biplots of the first two PCs for the log-, alr-, clr – and ilr- transformed data using classical PCA.

Element relations that are resulted from the log- and alr- transformed data are similar to those yielded by the clr- and ilr-transformed data (Table 3). For example, the Au (-As-Sb) relation with PC5 and PC4 for log- and alr-transformed data respectively is similar with PC1 of either the clr- or ilr-transformed data and hence these relations reflect the presence of gold mineralization in the study area. However, if the Kaiser (1960) criterion eigenvalues >1 is applied, an anomalous multi-element association reflecting the presence of gold mineralization in the study area is extracted only from either the clr- or ilr-transformed data but not from either the ln- or alr-transformed data (Table 3).

3.4. Maps of elemental association anomalies

In the previous section, it was shown that the ln- and alr- transformed data represent multi-element association anomalies (associated with mineral deposit occurrence) that do not explain the substantial proportion (i.e., eigenvalues >1) of the total variance in the data. In order to examine and map multi-element association anomalies extracted from the log- and alr- transformed data compared with multi-element association anomalies extracted from the clr- and ilr- transformed data, PC scores representing element association anomalies in the individual datasets are subjected to C-A fractal analysis.

The PC5 and PC4 of the log- and alr-transformed data (representing Au-As-Sb anomalies) and PC2 of the clr-transformed data (representing Au-As-Sb anomalies) and negated PC1scores of the ilr-transformed data (representing Au-Cu anomalies) (Table 3) can

95

be divided into five classes according to four inflection points in the C-A plots (Fig. 6). These five classes are considered, with respect to the known Au deposit occurrences, to show low-background, high-background, low-anomaly, high-anomaly and extremely high-anomaly (Fig. 6).
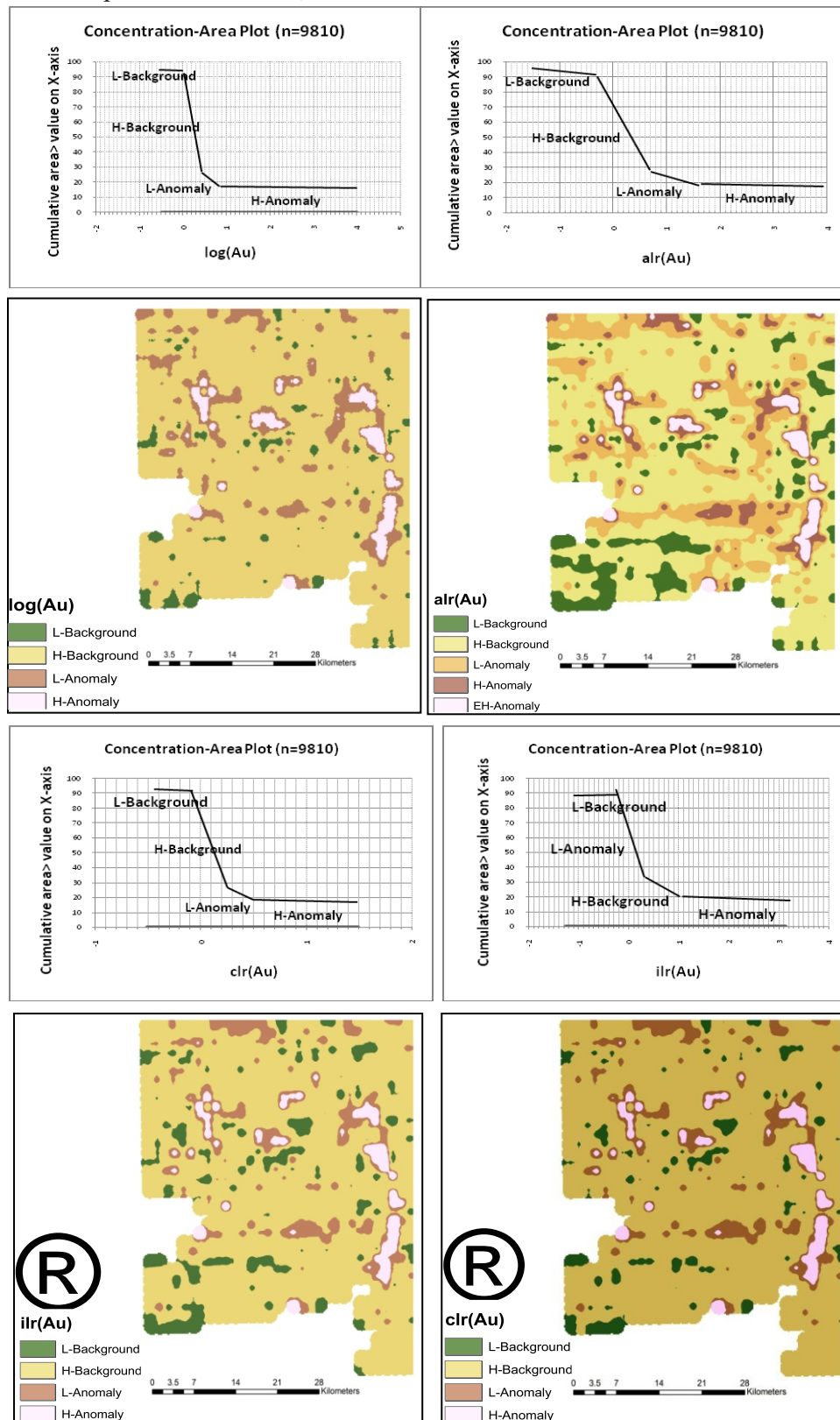

Fig.6. PC scores vs. area plots of anomalous multi-elements of log-, alr-, clr- and ilr- transformed multi-element data and the corresponding classified anomaly maps according to inflection points of concentration-area plots (solid dots) along straight-line segments fitted through the plots. L=low, H=high, EH=extremely high.

The anomaly maps obtained from the log- and alr- transformed multi-element data are similar to each other but the area of anomalies in alr-transformed multi-element map is more than the area of anomalies in log-transformed multi-element map. The anomaly maps obtained from the clr- and ilr- transformed multi-element data are also strongly similar to each other. Anomalies in the first maps are quite different from those in the latter maps (Fig. 7). For comparison with the ground-truth anomaly map (Fig. 3), the anomaly classes are re-classified into a single anomaly class and the background classes. The anomaly maps of the clr- and ilr-transformed multi-element data have higher OAs and the lower T2Es than those obtained from the log- and alr-transformed multi-element data (Table 4). Accordingly, the values of OA for the anomaly maps based on log-, alr-, clr-, and ilr- transformed multi-element data are 0.63, 0.74, 0.90 and 0.90, respectively (Table 4).

4. Conclusion

Geochemical data are compositional and thereby closed data. Mathematically they define points in the Aitchison geometry on the simplex and not in the usual Euclidean space for which all classical statistical methods are designed. For this reason, all calculations which are based on Euclidean distances give misleading results.

The obtained results of OA values, showed that logratio (alr, clr, or ilr) transformations, compared to log-transformation of stream sediment geochemical data improve mapping of Au anomalies reflecting presence of mineralization. In particular, clr- or ilr-

Table 4. Overall accuracy (OA), Type I and Type II errors (T1E and T2E, respectively) with respect to ground-truth background-anomaly map (Fig.3) of binary background-anomaly maps obtained from PC analysis of ln-, alr-, clr- and ilr-transformed Au data. Values in the matrix are number of samples of overlap condition between two binary anomaly-background maps.

log-transformed Au		Ground-truth		alr-transformed Au			Ground-truth	
		Anomaly	Background				Anomaly	Background
Results of analysis	Anomaly	31	297	Results of analysis	Anomaly		55	245
	Background	83	621		Background		15	718
	T1E=0.28	T2E=0.48			T1E=0.21		T2E=0.25	
	OA=0.63				OA=0.74			

clr-transformed Au		Ground-truth		ilr-transformed Au			Ground-truth	
		Anomaly	Background				Anomaly	Background
Results of analysis	Anomaly	81	128	Results of analysis	Anomaly		106	120
	Background	9	815		Background		12	795
	T1E=0.90	T2E=0.14			T1E=0.90		T2E=0.13	
	OA=0.87				OA=087			

These indicate that either the clr- or ilr- transformed multi-element data are suitable and sufficient for mapping of multi-element anomalies using the C-A fractal analysis, so, these transformations result in the optimum mapping of multi-element anomalies using the C-A fractal analysis.

transformed stream sediment geochemical data generally result in the best anomaly maps of Au in the study area.

Also, the results of the study imply that in regional-scale stream sediment geochemical survey, applying either log- or alr-transformed data is prone to miss significant multi-element anomalies and stream sediment geochemical data should be clr- or ilr-transformed to enhance recognition of anomalous multi-element associations reflecting the presence of mineralization. This is a crucial merit because variations in trace element concentrations in regional-scale stream sediment geochemical data are mostly due to lithology and other factors or processes unrelated to mineralization.

References

Afzal, P., Khakzad, A., Moarefvand, P., RashidnejadOmran, N., Esfandiari, B., Fadakar Alghalandis, Y., 2010. Geochemical anomaly separation by multifractal modeling in Kahang (GorGor) porphyry system. Central Iran. Journal of Geochemical Exploration, 104, 34-46.

Agterberg,F.P., Cheng, Q., Wright, D.F., 1993. Fractal modeling of mineral deposits. In: Elbrond J, Tang X (eds.), 24th APCOM symposium proceeding, Montreal, Canada, 43–53.

Aitchison, J., 1981. A new approach to null correlation of proportions. Mathematical Geology, 13, 175-189.

Aitchison, J., 1983. Principal component analysis of compositional data. Biometrika, 1, 57-65.

Aitchison, J., 1984. The statistical analysis of geochemical compositions. Mathematical Geology, 16, 531-564.

Aitchison, J., 1986. The statistical analysis of compositional data. Chapman & Hall, London.

Aitchison, J., 1999. Logratios and natural laws in compositional data analysis. Mathematical Geology, 31, 563-589.

Aitchison, J., Barceló-Vidal, C., Martín-Fernández, J.A., Pawlowsky-Glahn, V., 2000. Logratio analysis and compositional distance, Mathematical Geology, 32, 271–2755.

Aitchison, J., Greenacre, M., 2002. Biplots of compositional data. Journal of Royal Statistic Society, 51(4), 375-392.

Bai, J., Porwal, A., Hart, C., Ford, A., Yu, L., 2010. Mapping geochemical singularity using multifractal analysis: application to anomaly definition on stream sediments data from Funin Sheet, Yunnan, China. Journal of Geochemical Exploration, 104, 1–11.

Behrouzi, A., 1987. Geological map of 1:100000 Feyzaabad, Sheet No.:7760, Geological Organization, Tehran, Iran.

Buccianti, A., Pawlowsky-Glahn, V., 2005. New perspective on water chemistry and compositional data analysis. Mathematical Geology, 37, 703-727.

Carranza, E.J.M., 2008. Geochemical anomaly and mineral prospectivety mapping in GIS. Handbook of exploration and environmental geochemistry. Elsevier, Amsterdam.

Carranza, E.J.M., 2011. Analysis and mapping of geochemical anomalies using logratio-transformed stream sediment data with censored values. Journal of Geochemical Exploration, 110(2), 167-181.

Cheng, Q., Agterberg, F.P., Ballantyne, S.B., 1994. The separation of geochemical anomalies from background by fractal methods. Journal of Geochemical Exploration, 54, 109-130.

Cheng, Q., Agterberg, F.P., Bonham-Carter, G.F., 1996. A spatial analysis for geochemical anomaly separation. Journal of Geochemical Exploration, 56, 183-195.

Cheng, Q., Bonham-Carter, G.F., Hall, G.E.M., Bajc, A., 1997. Statistical study of trace elements in the soluble organic and amorphous Fe-Mn phases of surficial sediments, Sudbury Basin,1, Multivariate and spatial analysis. Journal of Geochemical Exploration, 59, 27-46.

Cheng, Q., Xu, Y., Grunsky, E., 2000. Integrated spatial and spectrum method for geochemical anomaly separation. Natural Resources Research, 9, 43-52.

Daya, A.A., Afzal, P., 2015. A comparative study of concentration-area (CA) and spectrum-area (SA) fractal models for separating geochemical anomalies in Shorabhaji region, NW Iran. Arabian Journal of Geosciences, 1-13.

Deng, J., Wang, Q., Yang, L., Wang, Y., Gong, Q., Liu, H., 2010. Delineation and explanation of geochemical anomalies using fractal models in the Heqing area, Yunnan Province, China. Journal of Geochemical Exploration, 105, 95–105.

Eftekharnezhad J., Aghanabati A., Baroyant V., Hamzehpour, B., 1976. Geological Quadrangle Map of kashmar, 1: 250000, GIS, Tehran, Iran,

Egozcue,J.J., Pawlowsky-Glahn, V., 2005. Groups of parts and their balances in compositional data analysis. Mathematical Geology, 37, 795–828.

Egozcue, J.J., Pawlowsky-Glahn, V., Mateu-Figueraz, G., Barceló-Vidal, C., 2003. Isometric logratio transformations for compositional data analysis, Mathematical Geology, 35(3), 279-300.

Exploration Co. Jiangxi China, 1994. Explanatory text of geochemical map of Feizaabad (7760) Stream sediment survey 1:100000. Report No 22.

Filzmoser, P., Hron, K., Reimann, C., 2009a. Principal component analysis for compositional data with outliers. Environmetrics, 20, 621- 632.

Filzmoser, P., Hron, K., Reimann, C., 2009b. Univariate statistical analysis of environmental (compositional) data-problems and possibilities. Science of Total Environment, 407, 6100-6108.

Filzmoser, P., Hron, K., Reimann, C., 2012. Interpretation of multivariate outliers for compositional data. Computer Geosciences, 39, 77-85.

Gabriel, K.R., 1971. The biplot graphic display of matrices with application to principal component analysis. Biometrika, 58(3), 453-467.

Goldschmidt, V.M., 1937. The principles of distribution of chemical elements in minerals and rocks. Journal of Chemical Society, 655–673.

Hasanipak, A.A., Sharafaldin, M., 2004. GET: a function for preferential site selection of additional borehole drilling. Exploration and Mining Geology, 13(1-4), 139-146.

Hassanpour, S., Afzal, P., 2013. Application of concentration–number (C–N) multifractal modeling for geochemical anomaly separation in Haftcheshmeh porphyry system, NW Iran. Arabian Journal of Geosciences, 6, 957–970.

Heydari, A., 2011. Exploration report of Kuh Zar deposit in Torbat-e-Heydarieh area, Zarmehr mining company, 133.

Hosseini, S.A., Afzal, P., Sadeghi, B., Sharmad, T., Shahrokhi,S.V., Farhadinejad, T., 2014. Prospection of Au mineralization based on stream sediments and lithogeochemical data using multifractal modeling in Alut1:100,000 sheet, NW Iran. Arabian Journal of Geosciences, 8(6), 3867-3879.

Kaiser, H.F., 1960. The application of electronic computers to factor analysis. Education Psychological Measurements, 20, 141-151.

Lima, A., De Vivo, B., Cicchella, D., et al., 2003. Multifractal IDW Interpolation and Fractal Filtering Method in Environmental Studies: An Application on Regional Stream Sediments of (Italy), Campania Region. Applied Geochemistry, 18(12): 1853–1865.

Lindenberg, H.G., Gorler, K., Ibbeken, H., 1983. Stratigaphy, structure and orogenic evolution of the sabzevar zone in the area of oryan Khorasan, NE Iran, GSI, Rep. No. 51, 119-143, Tehran Iran.

Mandelbrot, B.B., 1983. The fractal geometry of nature. Freeman, San Francisco.

Mazloumi, A.R., Karimpour, M.H., Rassa, I., Rahimi, B., Vosoughi Abedini, M., 2008. Kuh-E-Zar Gold Deposit in Torbat-e-Heydaryeh, New Model of Gold Mineralization, Iranian Journal of Crystalography and Mineralogy, 16(3), 363-376.

Nazarpour, A., Sadeghi, B., Sadeghi, M., 2015. Application of fractal models to characterization and evaluation of vertical distribution of geochemical data in Zarshuran gold deposit, NW Iran. Journal of Geochemical Exploration, 148, 60-70.

Pawlowsky-Glahn, V., Egozcue,J.J., 2006. Compositional data and their analysis, an introduction; In Buccianti, A., Mateu-Figueras, G., Pawlowsky-Glahn, V.(Eds.), Compositional data analysis in the geosciences: from theory to practice. Geological Society, London.

Rahmati, A., Afzal,P., Abrishamifar, S.A., Sadeghi, B., 2014.Application of concentration – number and concentration–volume fractal models to

delineate mineralized zones in the Sheytoor iron deposit, Central Iran. Arabian Journal of Geosciences, 8(5), 2953-2965.

Reimann, C., Filzmoser, P., Fabian, K., Hron, K., Birke, M., Demetriades, A., Anna,E.D., 2012. —The concept of compositional data analysis in practice Total major element concentrations in agricultural and grazing land soils of Europe. Science of Total Environment, 426, 196-210.

Reimann, C., 2005. Geochemical mapping- technique or art?, Geochemistry: Exploration, Environment, Analysis, 5, 359-370.

R development Core team, 2008. R: a language and environment for statistical computing, Vienna. (http://www.r-project.org).

Sadeghi, B., Moarefvand, P., Afzal, P., Yasrebi, A.B., Daneshvar Saein, L., 2012. Application of fractal models to outline mineralized zones in the Zaghia iron ore deposit, Central Iran. Journal of Geochemical Exploration, 122, 9–19.

Shahi, H., Kamkar-Rouhani, A., 2014. A GIS- based weights-of-evidence model for mineral potential mapping of hydrothermal gold deposits in Torbat-e-Heydarieh area, Journal of Mining & Environment, 5(2), 70-89.

Sim, B.L., Agterberg, F.P., Beaudry, C., 1999. Determining the cutoff between background and relative base metal contamination levels using multifractal methods. Computational Geosciences, 25, 1023–1041.

Stöcklin, J., 1968. Structural history and tectonics of Iran, a review. American Association of Petroleum Geologists Bulletin, 52, 1229–1258.

Templ, M., Hron, K., Filzmoser, P., 2009. robCompositions: Robust estimation for compositional data. Manual and package, version, 1(4).

Thió-Henestrosa, S., Martín-Fernández, J.A., 2005. Dealing with compositional data: the freeware CoDaPack. Mathematical Geology, 37(7), 773-793.

Turcotte, D.L., 1986. A fractal approach to the relationship between oregrade and tonnage. Economical Geology, 18, 1525–1532.

Van den Boogart, K.G., Tolosana, R., Bren, M., 2009. Compositions: Compositional data analysis. R package version 1.01-1.

Wang, W., Zhao, J., Cheng, Q., 2014. Mapping of Fe mineralization-associated geochemical signatures using logratio transformed stream sediment geochemical data in eastern Tianshan, China. Journal of Geochemical Exploration, 141, 6-14.

Zuo, R., 2011. Identifying geochemical anomalies associated with Cu and Pb-Zn Skarn mineralization using principal component analysis and spectrum-area fractal modelling in the Gangdese Belt, Tibet (China). Journal of Geochemical Exploration, 111, 13–22.